Antiferromagnetic Solids

Deutsche Ausgabe: DOI: 10.1002/ange.201506869
Internationale Ausgabe: DOI: 10.1002/anie.201506869

Extending the Family of V^{4+} $S = 1/2$ Kagome Antiferromagnets

*Lucy Clark, Farida H. Aidoudi, Cameron Black, Kasun S. A. Arachchige, Alexandra M. Z. Slawin, Russell E. Morris, and Philip Lightfoot**

Abstract: *The ionothermal synthesis, structure, and magnetic susceptibility of a novel inorganic–organic hybrid material, imidazolium vanadium(III,IV) oxyfluoride $[C_3H_5N_2]$-$[V_9O_6F_{24}(H_2O)_2]$ (ImVOF) are presented. The structure consists of inorganic vanadium oxyfluoride slabs with kagome layers of V^{4+} $S = 1/2$ ions separated by a mixed valence layer. These inorganic slabs are intercalated with imidazolium cations. Quinuclidinium (Q) and pyrazinium (Pyz) cations can also be incorporated into the hybrid structure type to give QVOF and PyzVOF analogues, respectively. The highly frustrated topology of the inorganic slabs, along with the quantum nature of the magnetism associated with V^{4+}, means that these materials are excellent candidates to host exotic magnetic ground states, such as the highly sought quantum spin liquid. Magnetic susceptibility measurements of all samples suggest an absence of conventional long-range magnetic order down to 2 K despite considerable antiferromagnetic exchange.*

Geometrically frustrated magnets are crystalline solids in which the arrangement of spin moments prevents the long-range magnetic order that typically prevails in magnetic materials upon cooling. Instead, the frustration that can be imposed on the magnetic interactions within a material as a result of its structure leads to a wealth of unusual magnetic behaviors.[1] An archetypal geometrically frustrated structure is the kagome lattice, formed from a two-dimensional corner-sharing triangular network of magnetic ions. When the kagome lattice is dressed with a set of antiferromagnetically interacting $S = 1/2$ species, an exciting possibility presents itself: the realization of a quantum spin liquid (QSL).[2] The QSL is a long-sought-after magnetic phase of matter that was originally proposed as an alternative to the ordered Néel ground state of an antiferromagnet.[3] It has many intriguing properties, for instance, despite being a system of highly entangled correlated spins it can evade a conventional symmetry-breaking magnetic phase transition even at $T = 0$ K and instead may exhibit a topological order that could have important consequences for quantum information technology.[4] Furthermore, it can support the existence of unusual magnetic excitations known as spinons, which are relatively well understood in one-dimensional magnets but far less so for magnetic systems of higher dimensionality.[5] In two dimensions, the $S = 1/2$ kagome antiferromagnet is the prime candidate to host a QSL state.[6]

The challenge for chemists has been to synthesize materials that can realize the fascinating physical properties expected from QSL theory.[7] The main difficulty in achieving this goal lies in the need to control the many factors that, although interesting, may ultimately limit the usefulness of a material as an experimental realization of a QSL. Nevertheless, the field of highly frustrated quantum magnetism has benefitted hugely in recent years from the synthesis of a number of viable QSL candidates in the chemistry laboratory. To date, the most widely studied $S = 1/2$ kagome antiferromagnet is the Cu^{2+}-based mineral Herbertsmithite, $ZnCu_3(OH)_6Cl_2$, which has a rhombohedral structure that consists of kagome layers of Cu^{2+} $3d^9$ $S = 1/2$ ions that are ideally separated by diamagnetic Zn^{2+} ions along the *c*-axis.[8] Experimental studies on both polycrystalline and single crystal forms of Herbertsmithite have revealed several of the key characteristics of a QSL.[9] However, the exact nature of the QSL ground state in Herbertsmithite remains an open question, chiefly regarding whether or not the spinon excitation spectrum is gapped or gapless, and theories supporting both have been proposed and are hotly debated.[10] In fact, the limitations of our understanding of the QSL phase on the $S = 1/2$ kagome lattice of Herbertsmithite stem primarily from an issue of materials chemistry. It is known that there is a degree of disorder at the Zn^{2+} site within the structure of Herbertsmithite, and an occupation of this inter-layer site by weakly coupled Cu^{2+} ions can often mask the properties intrinsic to the kagome layers.[11] Lately, other Cu^{2+}-based minerals, such as Barlowite, $Cu_4(OH)_6FBr$ and Kapellasite, a metastable polymorph of $ZnCu_3(OH)_6Cl_2$, have been proposed as new mother compounds for $S = 1/2$ kagome antiferromagnets.[12] There are advantages in diversifying the crystal chemistry in these systems to control magnetic interactions leading to QSL behavior. For example, in Barlowite, the inter-layer site that separates the Cu^{2+} kagome planes is sufficiently large such that, in theory, it may be doped by diamagnetic 4d ions, for example $M = Sn^{2+}$ or Cd^{2+}, to produce isolated two-dimensional kagome layers within $MCu_3(OH)_6FBr$, without the problem of anti-site disorder that is observed in the Zn-paratacamite family of Herbertsmithite.

There is, therefore, still a demand for more, and different, realizations of $S = 1/2$ kagome antiferromagnets, which presents a continuing challenge to chemists. The first example of a V^{4+}-based $3d^1$ $S = 1/2$ kagome antiferromagnet, the inorganic–organic hybrid solid diammonium quinuclidinium vanadium(III,IV) oxyfluoride, $[NH_4]_2[C_7H_{14}N][V_7O_6F_{18}]$ (DQVOF), was recently reported.[13] The difficulty in preparing such a system arose from a lack of control over the final

[*] Dr. L. Clark, Dr. F. H. Aidoudi, Dr. C. Black, Dr. K. S. A. Arachchige, Prof. Dr. A. M. Z. Slawin, Prof. Dr. R. E. Morris, Prof. Dr. P. Lightfoot
School of Chemistry and EaStChem, University of St Andrews
St Andrews, Fife, KY16 9ST (UK)
E-mail: pl@st-andrews.ac.uk

Supporting information for this article is available on the WWW under http://dx.doi.org/10.1002/anie.201506869.

oxidation state of vanadium and the preference of V^{4+} to form one-dimensional spin chains and ladders rather than condensing into an extended two-dimensional magnetic framework.[14] The synthesis of DQVOF was achieved through the departure from traditional solvothermal preparative techniques and the employment of the method of ionothermal synthesis. Ionothermal synthesis makes use of ionic liquids as solvents, which have proved fruitful in the crystallization of many new phases owing to the variety of solvent chemistry that they can present in comparison to conventional molecular solvents.[15] Herein, we discuss how this ionothermal method has been extended to prepare a new family of hybrid solids that contain a kagome network of V^{4+} $3d^1$ $S = {}^1/_2$ ions.

The first member of this new series of hybrid solids to be prepared was the imidazolium vanadium(III,IV) oxyfluoride, $[C_3H_5N_2][V_9O_6F_{24}(H_2O)_2]$ (ImVOF). ImVOF was prepared by ionothermal synthesis at a temperature of 190 °C with 1-ethyl-3-methylimidazolium bis(trifluoromethylsulfonyl)imide as a solvent and imidazole as a structure-directing agent. The same ionic liquid was used in the preparation of DQVOF, and is thought to play a key role in stabilizing the V^{4+} oxidation state, as in other common solvent systems over reduction of the vanadium is an issue. The relatively elevated reaction temperature is also known to be important in increasing the dimensionality of the inorganic framework. Unlike DQVOF, which exists as small turquoise crystals, ImVOF crystallizes as dark-purple crystals with a plate-like morphology. Analysis of single-crystal X-ray diffraction data (see the Experimental Section) revealed that the structure of ImVOF consists of isolated inorganic triple layers of composition $[V_9O_6F_{24}(H_2O)_2]^-$ separated by organic imidazolium cations $[C_3H_5N_2]^+$ (Figure 1). The layers within the inorganic vanadium oxyfluoride slabs are constructed from two kagome layers containing exclusively V^{4+} ions connected by a buckled kagome middle layer of V^{4+} ions and a mixed valence V^{3+}/V^{4+} site, as can be seen in Figure 2a. The oxidation states of the five unique vanadium sites within the structure of ImVOF have been determined by a bond-valence sum analysis[16] of the crystal structure (see the Supporting Information) and lead to a vanadium composition $V^{4+}{}_8V^{3+}$ per formula unit.

From Figure 1, it can be seen that the vanadium ions in the top and bottom layers of the inorganic slabs (V1, V2, and V3) are capped by oxide ions with short vanadyl V=O bonds characteristic of the V^{4+} oxidation state. Each of these sites forms a network of distorted corner-sharing VOF_5 octahedra in the *ab*-plane, which host the V^{4+} kagome layers. Within the middle layer there are two distinct vanadium sites. First, at the position labelled V4, a mixed-valence V^{3+}/V^{4+} site possesses a distorted octahedral $VF_5(H_2O)$ bonding environment, with dangling V–(OH_2) bonds at the apical position that alternate in the *ab*-plane. In the process of solving the crystal structure of ImVOF from single-crystal X-ray diffraction data, this dangling bond was initially assigned as V-F; however, allowing for an oxygen atom associated with a water molecule resulted in an overall improvement of the fit of the structural model to the data, a solution to an issue of non-physical anisotropic thermal parameters, a chemically sensible charge-balance for the compound overall, and a better agreement between calculated and experimentally determined CHN

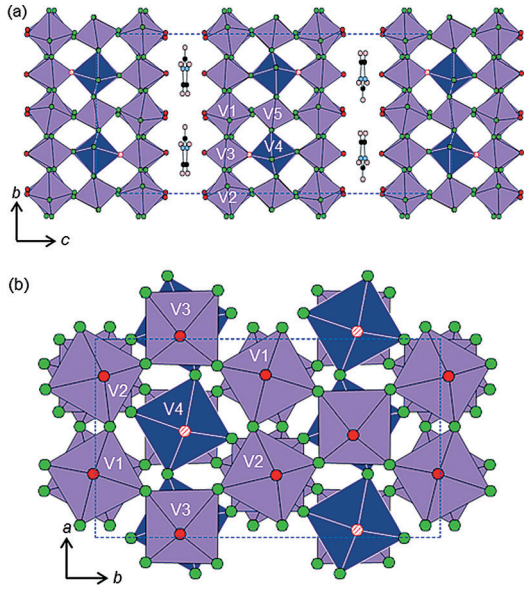

Figure 1. The crystal structure of ImVOF as viewed down the a) *a*-axis and b) *c*-axis. V^{4+} and mixed valence V^{3+}/V^{4+} sites are shown as light and dark polyhedra, respectively. Oxide ions red; fluoride ions green. Oxygen atoms of water are shown by the red hatched spheres. The imidazolium cations are shown in between the inorganic layers in (a).

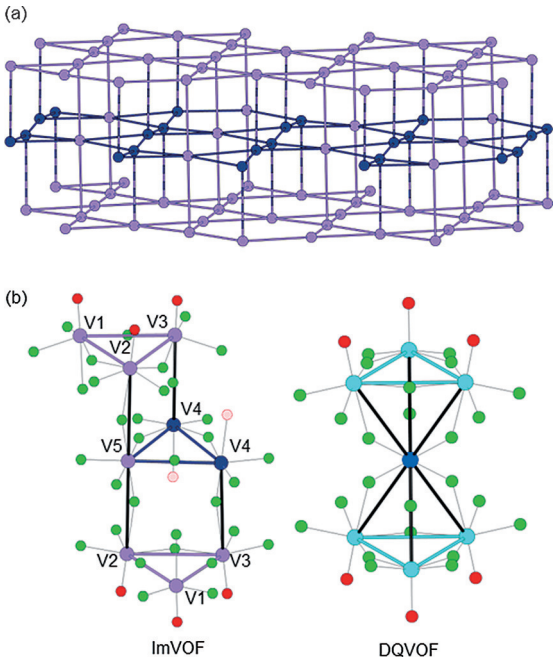

Figure 2. a) The tri-layer slabs of kagome-like networks in ImVOF with V^{4+} and V^{3+}/V^{4+} sites shown as light and dark purple, respectively. The V^{4+}-V^{4+} contact pathways are shown by light purple solid lines and those of V^{4+}-V^{3+}/V^{4+} by striped and dark purple. b) The connectivity between the vanadium species in ImVOF (left) and DQVOF (right). In DQVOF, the V^{4+} cations are shown as cyan and V^{3+} cations as dark blue. The connectivity between different vanadium species in adjacent layers, which are linked through bridging fluoride ions, is depicted by the solid black lines.

content (see the Supporting Information). The second vanadium site within the middle layer (V5) adopts the V^{4+} oxidation state within a VF_6 octahedron. These sites form a second kagome-like layer with the mixed valence V4 site buckled in and out of the *ab*-plane, as shown in Figure 2a.

It is instructive to consider the connectivity between the V^{4+} kagome layers and the mixed valence middle layer, and to compare this with the structure of DQVOF. Figure 2b shows that one of the sites (V1) within the V^{4+} kagome layers is not connected to the middle layer along the *c*-axis and is only coupled to the other two V^{4+} sites in the kagome plane through the corner-sharing of VOF_5 octahedra. The V3 site is coupled to one of the mixed valence sites within the middle layer through bridging fluoride ions, but this coupling is cut off on the opposite side of its octahedron along the *c*-axis by the dangling apical $V-(OH_2)$ bonds. It is only through corner-sharing of the octahedra belonging to the V2 and V5 centers along the *c*-axis that the two V^{4+} kagome layers are connected through the middle layer. This is considerably different from the structure of DQVOF. As shown in Figure 2b, the basic structural unit within the inorganic vanadium oxyfluoride layers of DQVOF is a double layer of V^{4+} kagome networks linked through bridging fluoride ions to a single V^{3+} $3d^2$ $S=1$ ion, resulting in a pyrochlore-slab geometry. In this way, the inorganic framework of DQVOF is reminiscent of the structure of Cu^{2+}-based Herbertsmithite, where the inter-plane V^{3+} site in DQVOF is analogous to the inter-plane Zn^{2+} site in Herbertsmithite. In contrast, the nature of the inter-layer bridging in ImVOF resembles the arrangement in a hexagonal tungsten bronze based on corner-sharing (albeit with dangling bonds rather than full connectivity) as opposed to the face-sharing, pyrochlore-like arrangement.[17] The fact that the connectivity between the $S=1/2$ kagome layers in ImVOF is so unlike that of the other available QSL candidate kagome materials is intriguing as it promises a potentially unique insight into the magnetic properties of such systems.

A detailed study of the low-temperature magnetic behavior of DQVOF revealed it to be a good candidate material for the realization of a QSL state. Despite the nearest-neighbor antiferromagnetic exchange, $J \approx 60$ K within the V^{4+} kagome layers, DQVOF demonstrates an absence of long-range magnetic order and spin freezing to at least 20 mK.[18,19] The V^{4+} kagome layers within the framework of DQVOF are thought to be reasonably well isolated from each other, which is due to a poor orbital overlap that mediates superexchange with the intermediate V^{3+} ions; the single t_{2g} electron associated with the $S=1/2$ V^{4+} ions within the kagome layers are localized in a d_{xy}-type orbital as a result of the orbital degeneracy of the $3d^1$ electron configuration in an octahedral crystal field. These half-filled d_{xy}-type orbitals are oriented perpendicular to the long V–F bonds that connect each V^{4+} ion to the V^{3+} inter-plane site. Evidence for this magnetic model is borne out in experimental studies of DQVOF, with paramagnetic, free-spin behavior of the $S=1$ spins of the V^{3+} ions observed in magnetization and heat capacity data at low temperatures.[18] However, whether or not, and how, these weakly coupled $S=1$ inter-plane spins affect the nature of the QSL phase of the $S=1/2$ kagome layers remains to be fully understood, and so a detailed comparison of the magnetic properties of DQVOF with other V^{4+}-based kagome systems, such as ImVOF, is extremely valuable. Figure 3 shows the magnetic and inverse susceptibilities of ImVOF measured in a zero-field-cooled (ZFC) field-cooled (FC) cycle in a 5 T field, thus comparable to the magnetic susceptibility measurements reported for DQVOF.[18] A Curie–Weiss fit to the inverse susceptibility over the temperature range 50–300 K yielded a Weiss constant $\theta = -38.5(2)$ K and an effective magnetic moment $\mu_{eff} = 5.482(4)$ μ_B per formula unit. The negative sign of the Weiss constant indicates that the dominant magnetic exchange interactions are antiferromagnetic in nature. The magnitude of the Weiss constant is comparable to that observed for DQVOF, which implies that the energy scales of the exchange interactions in both systems are equivalent. This stems from the similar network geometries and superexchange pathways within the V^{4+} kagome layers: the V–V contacts and V-F-V superexchange angles in DQVOF are 3.60 Å and 3.75 Å and 132° and 147° and in ImVOF are 3.61 Å, 3.71 Å and 3.72 Å and 134°, 141° and 149°, respectively. The small reduction of the observed effective magnetic moment in comparison to the spin-only moment $\mu_{so} = 5.65$ μ_B expected for eight V^{4+} ions and one V^{3+} ion per formula unit can be attributed to the spin–orbit coupling effects that are known to result in a reduction of effective moment in V^{3+}.[18] In the context of the search for new QSL candidate materials, the magnetic susceptibility data shown in Figure 3 are promising. The data show no strong evidence for a long range magnetic ordering transition or any spin glassiness down to the lowest measured temperature of 2 K, despite the considerable energy scale of the antiferromagnetic exchange set by the Weiss constant. This gives a frustration index, $f = |\theta|/T_N$, of at least about 20, indicating strong spin frustration in ImVOF. At $T \approx |\theta|$, the susceptibility data begin to deviate from Curie–Weiss behavior. This may reflect the onset of short-range spin correlations but could also result from the dominance of potentially weakly coupled spins in the middle layer at lower temperatures, as is thought to be the case for DQVOF.[18]

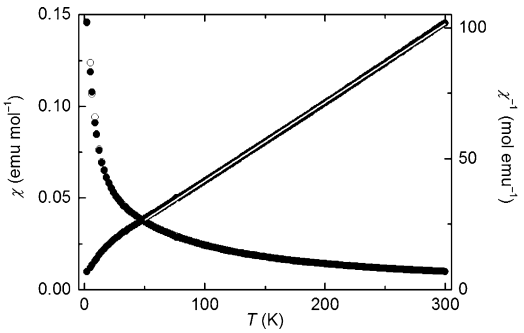

Figure 3. Magnetic (left) and inverse (right) susceptibilities of ImVOF measured in a 5 T field in a zero-field-cooled (●) field-cooled (○) cycle. The solid white line shows the Curie–Weiss fit applied to the inverse susceptibility data over the temperature range 50–300 K.

The ionothermal method used to prepare ImVOF has also been successful in the synthesis of two new related phases by varying the structure directing agent added to the reaction mixture. Quinuclidinium and pyrazinium vanadium oxyfluor-

ides, of idealized composition $[C_7H_{14}N][V_9O_6F_{24}(H_2O)_2]$ (QVOF) and $[C_4H_5N_2][V_9O_6F_{24}(H_2O)_2]$ (PyzVOF), have been prepared with quinuclidine and pyrazine, respectively, replacing imidazole in the synthetic procedure. This compositional diversity contrasts with DQVOF, where the use of quinuclidine as a structure directing agent appears to be critical for the crystallization of a kagome phase.[13] In the formation of DQVOF there is also partial breakdown of the quinuclidine to form NH_4^+ in situ, which is required to stabilize the specific nature of the pillared pyrochlore-like double layer; no secondary intra- or interlayer templating species are apparent in the present family. Hence, the ImVOF structure type is able to incorporate other template cations into its structure more easily, offering an extra variable through which to control the structure of these materials. Powder X-ray diffraction data of QVOF and PyzVOF, both of which have the same purplish hue as ImVOF, show that they crystallize with the orthorhombic $C222_1$ structure solved for single crystals of ImVOF. Furthermore, preliminary refinement of single crystal data for QVOF shows that the connectivity within the inorganic slab remains unchanged upon substitution of the organic template. Rietveld refinement of the orthorhombic structural model to the powder X-ray diffraction data reveals a variation of the room-temperature lattice constants as a function of the structure directing agent (see the Supporting Information) with increased lattice dimensions, particularly along the *c*-axis, arising in QVOF and PyzVOF owing to the bulkier nature of the quinuclidine and pyrazine templates in comparison with imidazole. The magnetic susceptibility data of QVOF and PyzVOF (see the Supporting Information) are consistent with that of ImVOF and reflect the highly frustrated geometry of the vanadium kagome network. Owing to their similar structure and magnetic responses ImVOF, QVOF, and PyzVOF can be considered as a new family of V^{4+} $S = {}^1/_2$ kagome antiferromagnets.

The crystal structure presented herein for the hybrid solid, ImVOF, consists of triple vanadium oxyfluoride slabs separated with imidazolium cations. The inorganic slabs are constructed of two V^{4+} $S = {}^1/_2$ kagome layers separated by a mixed-valence V^{3+}/V^{4+} buckled kagome middle layer. The magnetic susceptibility data presented for ImVOF show that, in spite of the dominance of antiferromagnetic exchange correlations, the spins within the system do not appear to order or freeze down to at least 2 K, a possible reflection of its highly frustrated topology. As such, ImVOF is a highly promising material and only the second of its kind, namely a realization of an $S = {}^1/_2$ kagome antiferromagnet based on V^{4+} $3d^1$ ions. The first example of such a material, DQVOF, also possesses a layered crystal structure, but the connectivity between the V^{4+} kagome layers is considerably different. A detailed comparison of the magnetic responses of ImVOF and DQVOF in the future will be important in furthering our understanding of the magnetic ground states of these systems, and in particular how the inter-layer spins interact with and affect the QSL state. We have also shown that, unlike DQVOF, this new structure is capable of hosting different organic structure-directing agents, with the ImVOF-type structure confirmed in the quinuclidine- and pyrazine-templated analogues, QVOF and PyzVOF, by Rietveld refinement of the ImVOF structural model to powder X-ray diffraction data. This powder-diffraction study revealed that the QVOF and PyzVOF analogues have an elongated *c*-axis compared to ImVOF, which results from a larger separation of the inorganic slabs. Both QVOF and PyzVOF also show an absence of spin order down to at least 2 K, and therefore a careful investigation of the low-temperature spin dynamics by, for example, muon spin relaxation (μSR) measurements will be necessary to determine whether the properties of the potential QSL state can be tuned as a function of the structure directing agent.[20] A recent μSR study of both of these systems revealed an absence of spin order and spin freezing down to at least 40 mK, which will be reported in a future publication from our group. Furthermore, the fact that this family of hybrid solids demonstrates the ability to host a variety of structure directing agents may allow for synthetic deuteration of these new materials with greater ease than is the case in DQVOF. In turn, this would permit the first neutron scattering studies of these systems, which could prove key in developing our understanding their unusual magnetic properties.

Experimental Section

Teflon-lined stainless steel autoclaves were charged with VOF_3 (1 mmol), organic template (0.5 mmol), HF (2.45 mmol, 40% in H_2O) and ionic liquid (5 mmol). The autoclaves were sealed and heated at 190 °C for 24 h. Once cooled, the products were filtered and washed with methanol and left to dry in air. In each case, purple-colored plate-like crystals were recovered. The essential difference between the syntheses of these new phases and that of DQVOF is the amount of organic template, as VOF_3 and $C_4H_{13}N$ are added in a 1:1 molar ratio in the preparation of DQVOF. It is this presence of a greater proportion of quinuclidine in the reaction mixture of DQVOF that results in the partial breakdown of the organic template, which in turn promotes the pillared double-layer structure of DQVOF.

Single-crystal X-ray diffraction data for ImVOF were collected on a Rigaku rotating anode diffractometer with Mo K_α radiation. The structure was solved by direct methods and refined against F^2 using the WinGX software to give $R1 = 0.0945$, $wR2 = 0.2123$, and a goodness-of-fit = 1.148. $Z = 4$, $M_r = 1115.58\ g\,mol^{-1}$, orthorhombic space group $C222_1$, $a = 7.3960(3)$ Å, $b = 12.7930(5)$ Å, $c = 28.523(1)$ Å, $V = 2698.8(2)$ Å^3, $\rho = 2.746\ g\,cm^{-3}$, $F(000) = 2112.0$, $\lambda = 0.71073$ Å, $T = 93$ K, $\mu = 3.17\ mm^{-1}$, 2433 reflections and $R_{int} = 0.1299$. Powder X-ray diffraction data were collected at room temperature on a STOE STADIP diffractometer with monochromated Cu $K_{\alpha 1}$ radiation. Samples were ground in a mortar and pestle and packed into a 0.5 mm outer-diameter quartz capillary, mounted, and aligned in the X-ray beam with data taken in Debye–Scherrer mode. Powder X-ray diffraction data were analyzed in terms of the Rietveld method using the GSAS software (see the Supporting Information).

Magnetic susceptibility data were taken on a Quantum Design MPMS SQUID magnetometer in zero-field-cooled (ZFC) field-cooled (FC) cycles over the temperature range 2–300 K in a 5 T field. The inverse magnetic susceptibilities were analyzed in terms of the Curie–Weiss law, $\chi^{-1} = (T-\theta)/C$, where θ and C are the Weiss and Curie constants, respectively. Fitting the inverse susceptibility of ImVOF over the temperature range 50–300 K gave $\theta = -38.5(2)$ K and $C = 3.757(3)\ emu\,mol^{-1}\,K$, which corresponds to an effective magnetic moment of 5.482(4) μ_B per formula unit, and $R^2 = 0.99989$. Equivalent fits of the inverse susceptibility data of QVOF and PyzVOF yielded $\theta = -26.9(7)$ K, $C = 3.98(1)\ emu\,mol^{-1}\,K$, $\mu_{eff} = 5.63$-

(1) μ_B, and $R^2 = 0.99864$ and $\theta = -25.5(1)$ K, $C = 3.643(2)$ emu mol^{-1} K, $\mu_{eff} = 5.400(3)\,\mu_B$, and $R^2 = 0.99995$, respectively (see the Supporting Information). Subsequent magnetic susceptibility measurements in a weaker applied field of 0.01 T were performed on all three systems and are shown in the Supporting Information.

The research data supporting this application can be accessed at http://dx.doi.org/10.17630/a9e4ddac-ea3b-46fc-b70c-d64efbc21546. CCDC 1421587 contains the supplementary crystallographic data for this paper. These data can be obtained free of charge from The Cambridge Crystallographic Data Centre.

Acknowledgements

We gratefully acknowledge funding support from The Leverhulme Trust (RPG-2013-343) and EPSRC (EP/K005499/1).

Keywords: crystal growth · fluorides · magnetic properties · vanadium · X-ray diffraction

How to cite: *Angew. Chem. Int. Ed.* **2015**, *54*, 15457–15461
Angew. Chem. **2015**, *127*, 15677–15681

[1] J. E. Greedan, *J. Mater. Chem.* **2001**, *11*, 37.
[2] L. Balents, *Nature* **2010**, *464*, 199.
[3] P. W. Anderson, *Mater. Res. Bull.* **1973**, *8*, 153.
[4] H.-C. Jiang, Z. Wang, L. Balents, *Nat. Phys.* **2012**, *8*, 902.
[5] B. Lake, D. A. Tennant, J.-S. Caux, et al., *Phys. Rev. Lett.* **2013**, *111*, 137205.
[6] C. Lhuillier, G. Misguich in *Introduction to Frustrated Magnetism* (Eds.: C. Lacroix, P. Mendels, F. Mila), Springer, Berlin, **2011**, pp. 23–41.
[7] A. Harrison, *J. Phys. Condens. Matter* **2004**, *16*, S553.
[8] M. P. Shores, E. A. Nytko, B. M. Bartlett, D. G. Nocera, *J. Am. Chem. Soc.* **2005**, *127*, 13462.
[9] a) P. Mendels, F. Bert, M. A. de Vries, et al., *Phys. Rev. Lett.* **2007**, *98*, 077204; b) A. Olariu, P. Mendels, F. Bert, et al., *Phys. Rev. Lett.* **2008**, *100*, 087202; c) M. A. de Vries, J. R. Stewart, P. P. Deen, et al., *Phys. Rev. Lett.* **2009**, *103*, 237201; d) T.-H. Han, J. S. Helton, S. Chu, et al., *Nature* **2012**, *492*, 406.
[10] a) S. Yan, D. A. Huse, S. R. White, *Science* **2011**, *332*, 1173; b) M. Hermele, Y. Ran, P. A. Lee, X. G. Wen, *Phys. Rev. B* **2008**, *77*, 224413.
[11] M. A. de Vries, K. V. Kamenev, W. A. Kocklemann, J. Sanchez-Benitez, A. Harrison, *Phys. Rev. Lett.* **2008**, *100*, 157205.
[12] a) T.-H. Han, J. Singleton, J. A. Schlueter, *Phys. Rev. Lett.* **2014**, *113*, 227203; b) R. H. Colman, C. Ritter, A. S. Wills, *Chem. Mater.* **2008**, *20*, 6897; c) B. Fåk, E. Kermarrec, L. Messio, et al., *Phys. Rev. Lett.* **2012**, *109*, 037208.
[13] F. H. Aidoudi, D. W. Aldous, R. J. Goff, et al., *Nat. Chem.* **2011**, *3*, 801.
[14] a) D. W. Aldous, N. F. Stephens, P. Lightfoot, *Dalton Trans.* **2007**, 4207; b) K. Adil, M. Leblanc, V. Maisonneuve, P. Lightfoot, *Dalton Trans.* **2010**, *39*, 5983; c) F. Himeur, P. K. Allan, S. J. Teat, et al., *Dalton Trans.* **2010**, *39*, 6018.
[15] R. E. Morris, *Chem. Commun.* **2009**, 2990.
[16] N. E. Brese, M. O′Keeffe, *Acta Crystallogr. Sect. B* **1991**, *47*, 192.
[17] K. K. Wandner, R. Hoppe, *Z. Anorg. Allg. Chem.* **1987**, *549*, 7.
[18] L. Clark, J.-C. Orain, F. Bert, et al., *Phys. Rev. Lett.* **2013**, *110*, 207208.
[19] J.-C. Orain, L. Clark, F. Bert, et al., *J. Phys. Conf. Ser.* **2014**, *551*, 012004.
[20] M. O. Ajeesh, A. Yogi, M. Padmanabhan, R. Nath, *Solid State Commun.* **2015**, *207*, 16.

Received: July 24, 2015
Revised: September 28, 2015
Published online: October 30, 2015

